



Journal of Mining and Environment (JME)

journal homepage: www.jme.shahroodut.ac.ir



CFD-based Modeling of Sarin Gas Dispersion in a Subway Station—A Hypothetical Scenario

Mohammad Hosseini, Hassan Madani* and Kourosh Shahriar

Department of Mining Engineering, School of Petroleum, Civil and Mining Eng, Amirkabir University of Technology, Tehran, Iran

Article Info

Received 26 January 2022

Received in Revised form 4 March 2022

Accepted 9 March 2022

Published online 9 March 2022

[DOI:10.22044/jme.2022.11604.2150](https://doi.org/10.22044/jme.2022.11604.2150)

Keywords

Sarin

Chemical attack

CFD

Subway station

Piston effect

Abstract

The main purpose of this work is modeling the dispersion of the sarin gas in a subway station in a hypothetical scenario. The dispersion is modeled using the CFD approach. In the analysis of the environmental conditions of the underground spaces, the only factor that draws a distinction between a subway station and other spaces is the train piston effect. Therefore, the present research work models the sarin dispersion in the two general cases of with and without a train in the subway system. About 0.5 L of sarin is assumed to be released through the main air handling unit (AHU) of the station. The results obtained show that in the case with no train service in the station, after 20 minutes of sarin release, the concentration and dose of sarin in the station will be 8.9 mg/m³ and 80 mg minute/m³, respectively, and these values are highly dangerous and lethal, and would have severely adverse effects on many individuals, and lead to death. This is highly important, especially when the effect of ventilation chambers at the ground level is taken into consideration. The results obtained also show that the train piston effect reduces the concentration and dose of sarin in the station so that when train arrival at and departure from the station, the sarin dose considerably reduces to 25 mg min/m³ after the release, and contributes to lower casualties. Finally, the results obtained show that time is a key factor to save lives in the management of such incidents.

1. Introduction

Having become the transportation mode of choice in many countries worldwide, the subway systems are now considered as one of the most important assets of the modern societies. A subway system consists of five main components, namely tunnels and lines, stations and facilities, trains, telecommunications and monitoring, and energy supply facilities, among which the stations are the most important component [1]. Unfortunately, despite the advances in construction and maintenance, the stations are always vulnerable to natural and man-made hazards. Since the subway stations are densely crowded and have a limited space, any incident in these areas can lead to a disaster. The hazards threatening the stations can be categorized into the individual and social hazards. While the individual hazards threaten the life of one or very few individuals, the social

hazards affect many people's lives. Due to the severity of their impact and consequences, the social hazard is more important to be analyzed compared with the individual hazards.

Terrorist attacks are the most important social hazards, as they not only cause loss of life and property damage but also lead to a secondary damage such as psychological disorders in the victims, security issues, loss of international reputation, and several social problems in general. For instance, about 25 years after the subway terrorist incident in Tokyo, Japan, many of the victims are still suffering from the psychological consequences of the incident [2].

Figure 1 shows the share of terrorist attacks in the subway stations and their respective share of casualties. It was observed that although only 2 of the 42 recorded incidents were chemical attacks

✉ Corresponding author: Hmadani@aut.ac.ir (H. Madani).

(4.7 %), they led to 6000 people (59.1 %) being killed or injured, indicating a high susceptibility of the subway stations to such incidents.

The Tokyo subway sarin attack is one of the most unpleasant recorded terrorist incidents in the subway stations and the largest incident in Japan after the Second World War, which produced more than 6000 victims. In 1995, five members of a terrorist group released sarin gas during the rush hour in a total of five subway lines of Tokyo. In this terrorist attack, most commonly antidote that used in hospital was unable to prevent CNS (central nervous system) damage, and no other oximes have been approved for use in Japan. Ultimately, 12 people died, and many victims had severe neurological injuries or sequelae [3]. A key reason behind the high casualties of chemical attacks is the unpreparedness of the subway systems against such incidents. A chemical agent can easily disperse inside a station without the authorities noticing or the station alarm systems detecting it. Only after many lives have been endangered can such dispersion be noticed [4].

Given the above, it can be concluded that a terrorist attack with chemical agents against a subway station is an attractive effortless choice for terrorists and saboteurs if raw materials are accessible.

This work analyzed the effects of chemical agent dispersion on environmental conditions in a subway station. In the analysis of the subway environments, the train piston effect should also be considered in addition to the ventilation systems of the station. In fact, as far as an analysis of their environmental conditions is concerned, the subway stations differ from other underground spaces only due to the train piston effect. On the other hand, there are several scenarios and choices for chemical attacks on the subway stations. The type of chemical agent, place and method of its release, and amount of the agent are among the variables of a chemical attack. The scenario considered in the present work is the release of sarin through the ventilation facilities of the station. It was assumed that a bottle of sarin was emptied in the ventilation shaft of the station.

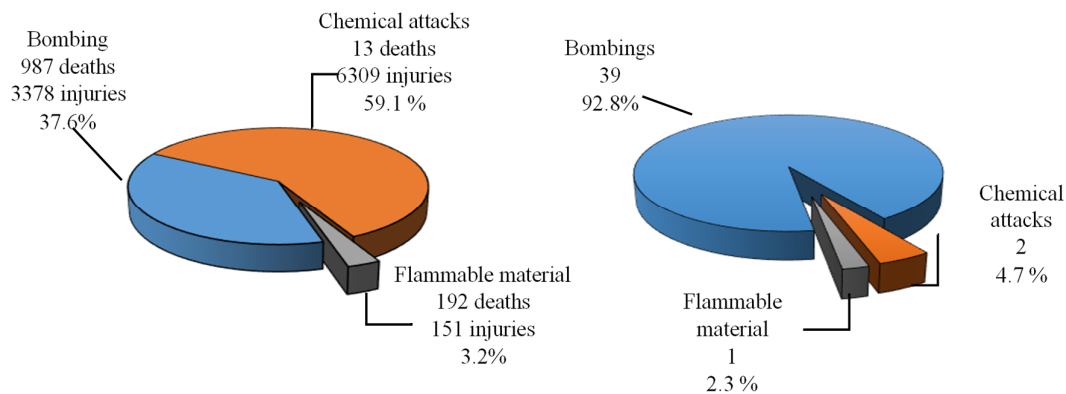


Figure 1. Share of terrorist attack fatalities and injuries in subway system.

The Tokyo subway attack in 1995 has been the subject of many publications, and various studies have been conducted on the dispersion of chemical agents and evacuation process in the underground spaces. The methods employed by these studies can be categorized into the measurement, mathematical, and computational fluid dynamic (CFD) approaches. Endregard et al. have used CFD and large eddy simulation (LES) approaches to model the sarin dispersion within an underground space in a hypothetical scenario. Their results indicated that serious injuries and fatalities occurred about 20 minutes after the initial release of sarin [5]. They also offered some evacuation plans and post-incident management approaches. Pflitsch et al. have analyzed the effects of natural

ventilation on the dispersion of toxic particles in the subway stations. They used sulfur hexafluoride (SF_6) as the tracer gas and climate data to analyze gas diffusion due to natural ventilation. Their results obtained showed that in many instances, the station escape routes were unsafe and contaminated with the gas particles [6]. In another study, Spiegel et al. have analyzed the effects of natural ventilation on the dispersion of chemical particles in a subway station. Their study was based on the dispersion of a tracer gas within a subway station in Newcastle, England. They found that in many instances, the passenger evacuation routes overlapped the gas diffusion pathways [7]. In a study by Gross, a particle dispersion model has been proposed to analyze the evacuation operations

for a subway station. This was a mathematical model based on the Monte Carlo simulation. Instead of considering the ventilation system of the station, Gross combined a uniform wind flow model based on the Navier-Stokes equations with a particle dispersion model. The results obtained showed that the designated escape routes were not always safe, and let through some of the contamination [8]. Widiatmojo et al. have modeled gas dispersion in a subway station. Their model was based on the particle tracking method, which considered discretized mass transfer based on the Brownian movement. This model was verified against the results from the tracer gas dispersion, and was shown to be reasonably accurate [9]. In a study by Brüne et al., the tracer gas sulfur hexafluoride was used to analyze dispersion of the chemical particles in a subway station with normal ventilation conditions. Their results indicated that the station exit routes were contaminated within minutes and harmed the passengers during evacuation [10]. Liang Ma et al. have used a Gaussian particle dispersion model, which is a mathematical model for particle dispersion in air, in order to model the dispersion of sarin in a hypothetical subway station. Their main objective was to analyze evacuation from the station during chemical attacks. In order to simplify the computations, they considered sarin to be vapor from the beginning of dispersion, and did not present a model for sarin evaporation [11]. Feng et al. have used computational fluid dynamics and agent-based simulation in order to evaluate and optimize the evacuation capacity of the subway station in Guangzhou, China. They analyzed the influence of the ventilation system on the gas diffusion process under different working conditions during simulations of the toxic gas

dispersion. Finally, the model of the impacts of the number of evacuees and individual risk perception levels on the evacuation risk has been obtained. Results indicate that the risk assessment and risk mitigation methods were effective and could help guide the emergency evacuation and ventilation system design for underground buildings [12]. Dolezal and Tomaskova have proposed an agent based model using the Anylogic software to model a part of the terrorist attack in the Tokyo subway in 1995 using sarin gas. They also used what-if scenarios to find the possibilities of minimizing the losses during attack [13].

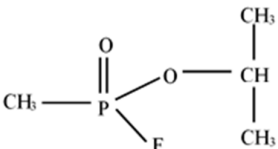
Based on the literature reviewed above, the present work used CFD to model sarin dispersion in a subway station. For this purpose, a probable scenario was first defined. Given the large size of the model geometry, the train piston effect was then calculated. The values obtained in this step were applied to the main problem as the boundary conditions. Finally, the dispersion of sarin in the station was modeled by taking into account the location of the train and its movement with respect to the system.

2. Description of Scenario

2.1. Type of dispersed chemical

Due to its toxicity, special physical properties, and use in the 1995 Tokyo subway incident, sarin was selected as the chemical of interest, and its dispersion in a subway station was modeled. The consequences of the Tokyo incident indicate that the subway stations are always vulnerable to sarin attacks. Table 1 presents the chemical and physical properties of Sarin. Table 2 shows the sarin toxicity for the general population based on the experimental data on animals.

Table 1. Chemical and physical properties of Sarin [14].

Names	Sarin, GB
Formula	C ₄ H ₁₀ FO ₂ P
Chemical structure	
Molecular weight	140.10
Physical state (20 °C)	Colourless liquid giving off a colourless vapor
Odor	Weak, fruity; almost none in pure state
Vapour density (compared to air)	4.86
Boiling point (°C, 760 mm Hg)	147–158
Melting point (°C)	-56
Volatility (mg/m ³)	6.091 at 20°

2.2. Specifications of subway station

A hypothetical mid-sized subway station was considered. The type and complexity of the building, its depth relative to the ground level,

ventilation systems, and other specifications were the same as those of a station in a standard conventional subway system. Accordingly, the hypothetical station had four exits leading up to ground level and four entrances to the platforms.

Table 2. Toxicity estimates for sarin for the 70 kg human [15].

Toxicity	Form of exposure	Exposure time (min)	Estimated value (mg min/m ³)	Minute volume (l min ⁻¹)
Mild effect	Inhalation, ocular and percutaneous	2-10	<2	-
EC _{t50} *(threshold effects)	Inhalation and percutaneous	2-10	2	15
EC _{t50} (mild effect)	Inhalation and percutaneous	2-10	25	15
LC _{t50} **	Inhalation and percutaneous	10	35	15
	Inhalation and percutaneous	2	60	15

* The dose that for exposure time, t, causes mild or threshold effects in 50% of the exposed population.

** The dose that for exposure time, t, produces lethal effects in 50% of the exposed population.

2.2.1. Building

The building of the station consisted of ticket halls, platforms, access corridors to the platforms,

and ground level. Figure 2 shows a 3D view of different parts of the station building with their respective dimensions.

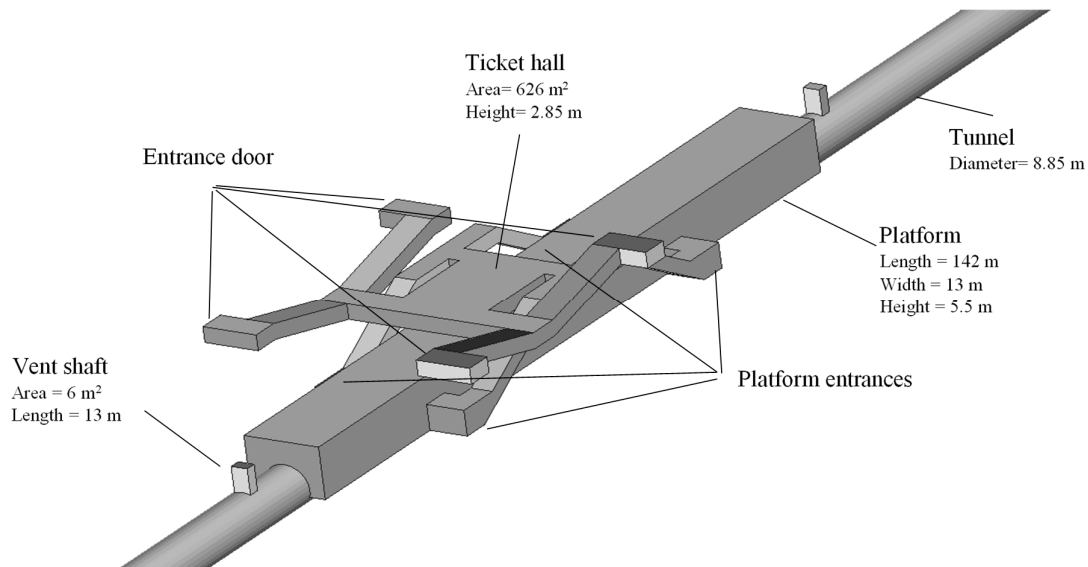


Figure 2. 3D view of different parts of station building.

2.2.2. Ventilation system

The ventilation system of the station is incorporated with tunnel vent shafts. Air flow produced by the main air handling unit (AHU) uniformly entered the station through ventilation channels built into the ceiling along the whole platform length. The tunnels were ventilated through the shafts located at both ends of the station and through the ventilation shaft in the

middle of the tunnel. Figure 3 presents a schematic view of the ventilation system. The tunnel vent shafts were 13 m long and had a square cross section of side 4.2 m. The specifications of the fan are given in Table 3. The air supplied by the main air handling unit (*Bl₁*) entered the platform area through a number of square ducts of side 0.5 m regularly placed at 1-m intervals along the length and width of the station.

2.2.3. Train

The train specifications are given in Table 4. The speed-time graph for the train movement in time

intervals from one station to the next is shown in Figure 4.

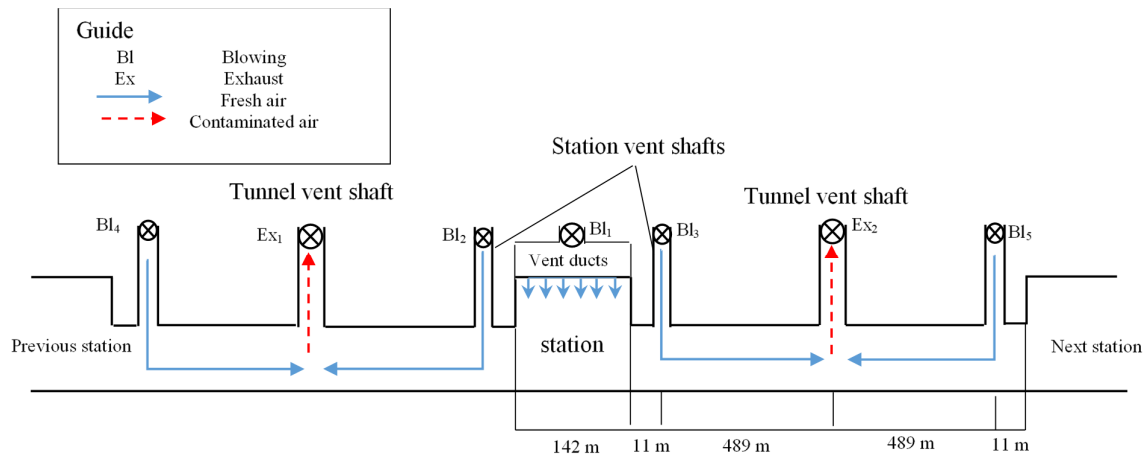


Figure 3. A schematic view of ventilation system.

Table 3. Specification of fans [16].

Fan number	Bl ₁	Bl ₂	Bl ₃	Bl ₄	Bl ₅	Ex ₁	Ex ₂
Pressure (Pa)	2700	720	720	720	720	350	350
Flow rate (m ³ /s)	50	20	20	20	20	80	80

Table 4. Subway train specification [16].

Length (m)	Width (m)	Height (m)	Head pressure loss coefficient	Tail pressure loss coefficient	Friction factor
140	2.6	3.5	0.25	0	0.03

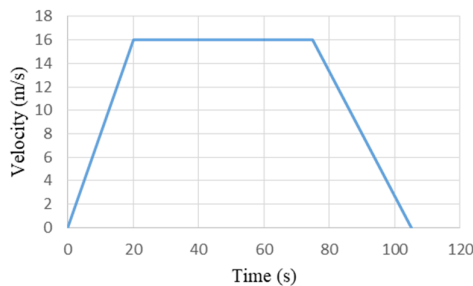


Figure 4. Velocity curve of subway train.

2.2.4. Release of chemical agent

Sarin was assumed to be released through the main air handling unit of the station. For simplification, it was assumed that sarin was poured in the ventilation chamber near the air distribution channel. It was also assumed that there was of liquid sarin in a cylindrical container of diameter 80 cm and height 2 mm.

2.2.5. Condition of train within system

As stated above, in the analysis of the environmental conditions, the only factor that draws a distinction between a subway station and other spaces is the train piston effect. Therefore, the present research work modeled sarin dispersion in the two general cases of with and without a train in the subway system.

3. Calculation of train piston effect

Due to the large amount of computation, it was impossible to model the train piston action and the sarin gas dispersion in the station simultaneously. This issue was resolved by dividing the main problem into two smaller ones: calculation of the train piston effect in a 3D simulation and modeling the sarin dispersion throughout the station. This was carried out by first calculating the train piston effect, determining the air velocity and pressure, and then applying their values as the boundary conditions to the problem of modeling the sarin dispersion. The train piston effect was calculated

through the dynamic layering method and a numerical model.

3.1. Mesh characteristics

In order to calculate the train piston action inside the tunnel, a model of the train in a tunnel was set up, and the location of the tunnel ventilation shafts

was made as the ceiling ducts so that the flow rate and pressure generated by the fans could be applied as the boundary conditions. A structured mesh was used for the whole geometry, and the computational grid was generated as a tetrahedral grid. The grid size in the tunnel was set to be 0.3 m, and the grid size adjacent to the train was set to be 0.2 m. Figure 5 depicts part of the tunnel grid.

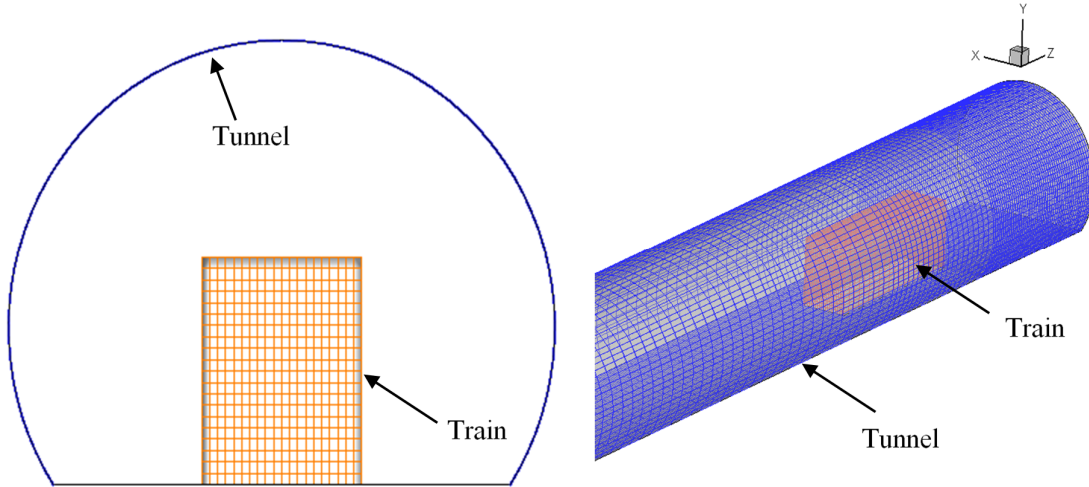


Figure 5. Solution domain and grid used.

3.2. Solver and numerical scheme

OpenFOAM (v. 1812) based on the finite volume method was employed for the computation. The equations governing the flow of a compressible fluid are continuity, momentum, and energy equations. The energy equation was neglected as the process was considered isothermal. For modeling flow turbulence, the Reynolds Average Navier-Stokes (RANS) equations were used along with the $k-\epsilon$ model. In some research works, the Reynolds-averaged Navier-Stokes (RANS) equations with standard $k-\epsilon$ turbulence model have been used to predict the train unsteady airflow, and the results were accurate [17], [18], [19] and [20]. The 3D Navier-Stokes equations for a compressible fluid are [21]:

- Continuity equation:

$$\frac{\partial \rho}{\partial t} - \frac{\partial \rho u_i}{\partial x_i} = 0 \quad (1)$$

- Momentum equation:

$$\frac{\partial \rho u_i}{\partial t} + \frac{\partial}{\partial x_i} (\rho u_i u_j) = - \frac{\partial p}{\partial x_i} + \frac{\partial}{\partial x_i} \left[(\mu + \mu_t) \left(\frac{\partial u_i}{\partial x_j} + \frac{\partial u_j}{\partial x_i} \right) \right] \quad (2)$$

- k equation:

$$\frac{\partial (\rho k)}{\partial t} + \frac{\partial}{\partial x_i} (\rho u_i k) = \frac{\partial}{\partial x_i} \left[\left(\mu + \frac{\mu_t}{\sigma_k} \right) \frac{\partial k}{\partial x_i} \right] + G - \rho \epsilon \quad (3)$$

- ϵ equation:

$$\frac{\partial (\rho \epsilon)}{\partial t} + \frac{\partial}{\partial x_i} (\rho u_i \epsilon) = \frac{\partial}{\partial x_i} \left[\left(\mu + \frac{\mu_t}{\sigma_\epsilon} \right) \frac{\partial \epsilon}{\partial x_i} \right] + C_{1\epsilon} \frac{\epsilon}{k} G - C_{2\epsilon} \rho \frac{\epsilon^2}{k} \quad (4)$$

where t is the time, u_i is the mean velocity component, ρ and μ are the density and viscosity coefficient of molecular, p is the pressure, and μ_t is the turbulent viscosity that is defined by the turbulent kinetic energy and turbulent dissipation rate as follows:

$$\mu_t = \rho C_\mu \frac{k^2}{\epsilon} \quad (5)$$

The standard set of constants adopted for the k and ϵ equations are as Table 5.

G is defined as:

$$G = \mu_t \left(\frac{\partial u_i}{\partial x_i} + \frac{\partial u_j}{\partial x_j} \right) \frac{\partial u_i}{\partial x_j} \quad (6)$$

and represents the generation term of the turbulent kinetic energy caused by the mean velocity gradient. The pressure–velocity coupling is taken care of by the PIMPLE algorithm.

Table 5. Standard set of constants in k and ε equations [21].

C_μ	σ_k	σ_ϵ	$C_{1\epsilon}$	$C_{2\epsilon}$
0.09	1	1.3	1.44	1.92

3.3. Boundary conditions

The boundary conditions in the problem are the ventilation shafts and the tunnel inlet and outlet. Based on Table 3, the injection shafts are defined with an inflow rate of 20 m³/s, and the extraction shaft is defined with an outflow rate of 80 m³/s. For the tunnel inlet and outlet, a static pressure condition was established with a value equal to the atmospheric pressure.

3.4. Dynamic mesh procedure

The train displacement was implemented using the dynamic layering method. The dynamic layering method is useful when the boundary displacement is large compared to the local cell sizes [22]. In the dynamic layering method, adding or removing the cell layers adjacent to a moving boundary is done based on the height of the layer adjacent to the moving surface. The layer of cells adjacent to the moving boundary is split or merged with the layer of cells next to it (layer *i*) based on the height (*h*) of the cells in layer (*j*) (Figure 6). Figure 7 shows the splitting and merging of the cells around the train.

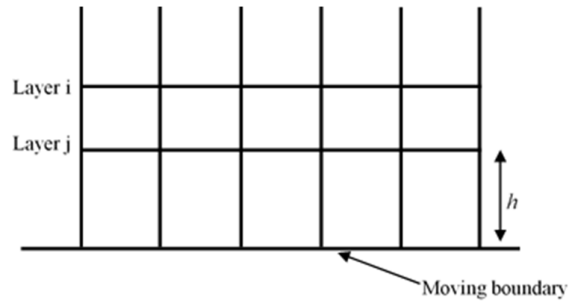


Figure 6. Dynamic layering method [22].

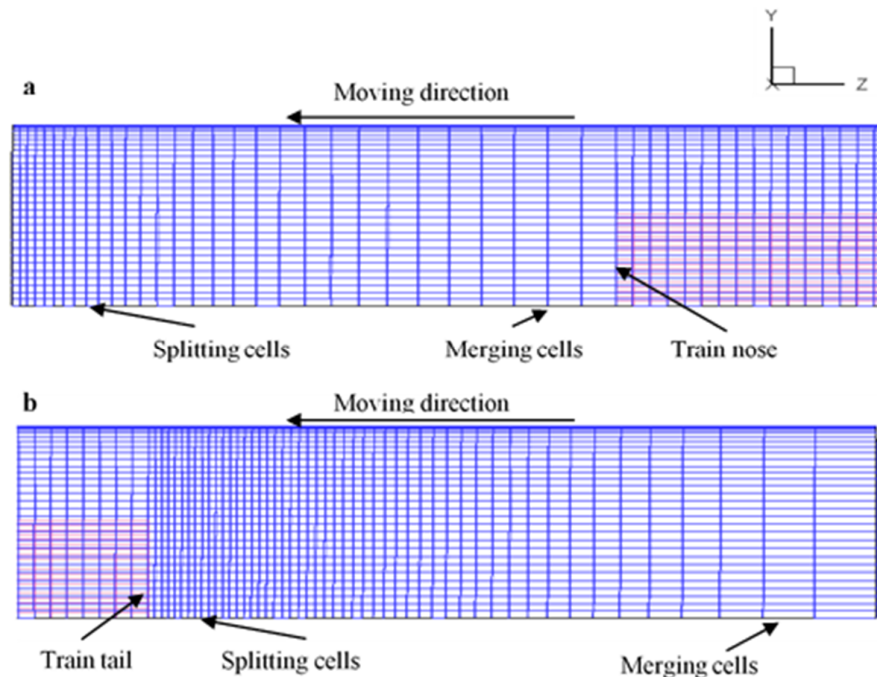


Figure 7. Splitting and merging of cells around train at : a. train nose, b. train tail.

3.5. Results

Figure 8 presents some of the results obtained from modeling the train piston effect. The figure shows the velocity and pressure contours around

the body of the train moving (Figure 8.a and Figure 8.b) and air streamlines around the train (Figure 8.c) at 14 m/s, 40 s after the train started moving. Due to this figure, in the region around the front of the train, the flow moves forward to the tunnel

outlet. In the region around the rear of the train, the flow coming from the front of the train spins back to the rear of the train, and the flow coming from the tunnel inlet to the rear of the train is made by the pressure drop in the rear of the train (Figure 8.c). Accordingly, when a train enters a station, the

positive pressure (based on Figure 8.b) in front of the train pushes some air in the tunnel flow into the platform of the station; similarly, when the train leaves the station, the negative pressure behind the train sucks the outdoor air into the tunnel (Figure 8.b).

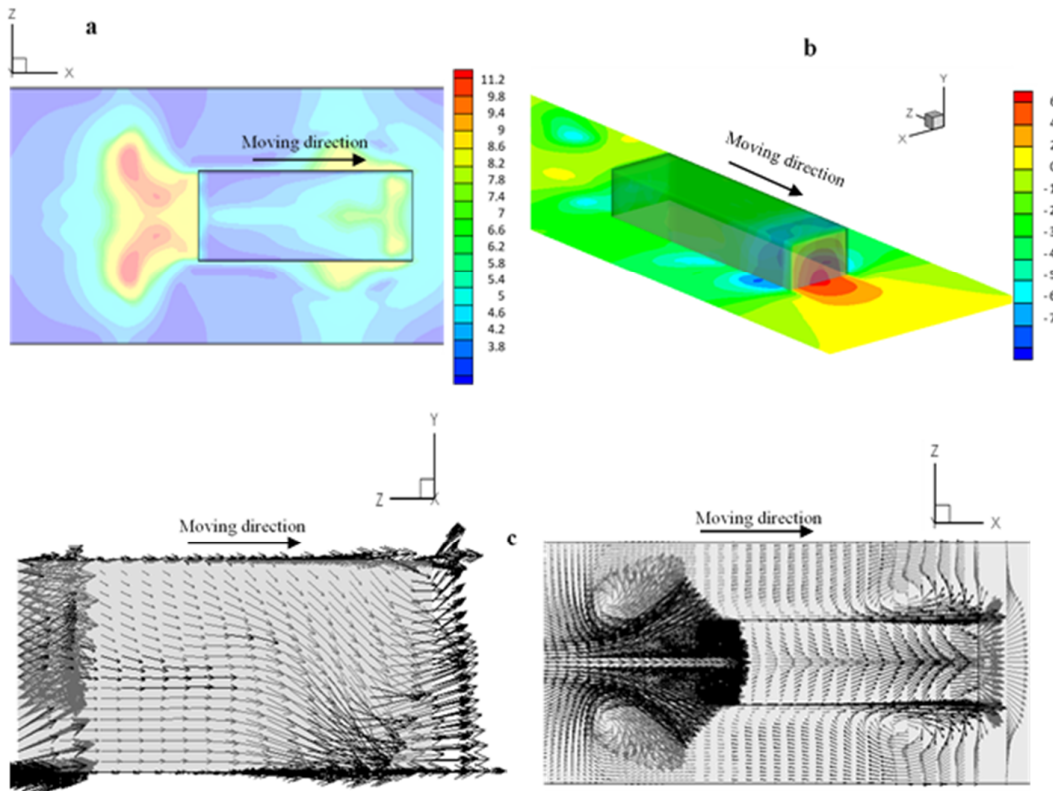


Figure 8. Characteristics of air around train at 14 m/s, 40 s after train started moving. a. Velocity contours b. Pressure contours c. Air streamlines

Figure 9 shows the graph of the rate of air flow through the station at train arrival and departure. The negative and positive values indicate the air flow sucked from and into the station, respectively.

The graph shows that the rate of air flow to the station peaked at 30 m³/s upon train arrival, while the rate of air flow from the station peaked at 58 m³/s upon train departure.

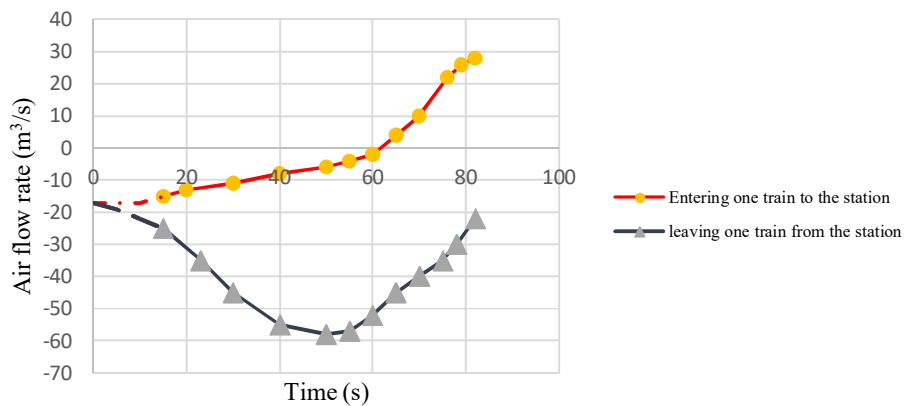


Figure 9. Air flow rate due to entering/leaving one train at station.

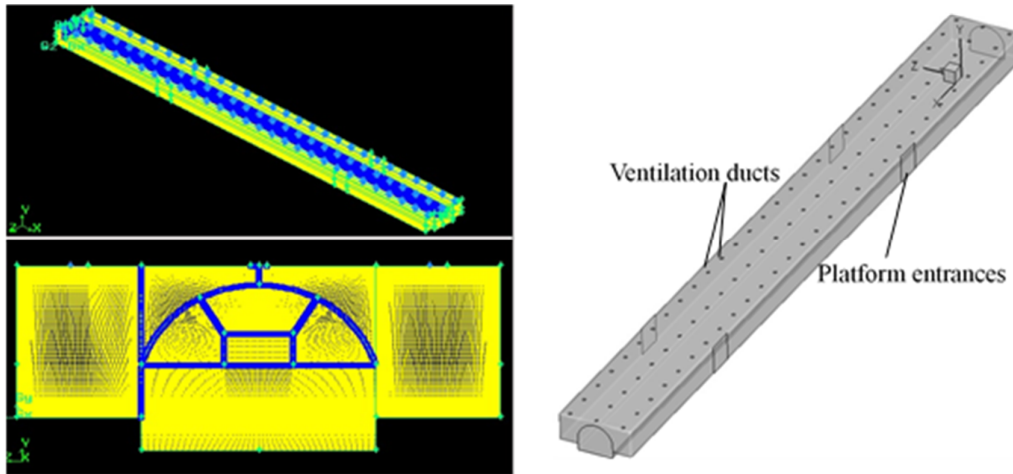


Figure 10. Calculation model of subway station.

4.2. Solver and numerical scheme

The equations governing the flow of a compressible fluid are the continuity, momentum, and energy equations. For modeling flow turbulence, the Reynolds Average Navier-Stokes

(RANS) equations were used along with the $k-\varepsilon$ model. The continuity and momentum equations and the $k-\varepsilon$ model are not discussed here, as they were already discussed in Section 3-1. The energy equation is written as [21]:

$$\frac{\partial}{\partial t}(\rho e_t) + \frac{\partial}{\partial x_i}(\rho u_i + p u_i) + \frac{\partial}{\partial y}(\rho v + p v) + \frac{\partial}{\partial z}(\rho w + p w) = \frac{\partial}{\partial x_i} [u_i \tau_{x_i x_j} - q_{x_i}] \quad (7)$$

where t is the time, u_i is the mean velocity component, ρ is the density, p is the pressure, τ is the shear stress, and q is the heat flux.

Since sarin was liquid when it was initially released in the ventilation system and gradually evaporated due to its high volatility, the problem was considered a two-phase flow (gas-liquid) problem. OpenFOAM (v. 1812) was used to solve the equations governing the fluid flow. The problem was set up as a two-phase model including the gas-liquid flow. The free surface flow consisted of two immiscible fluids divided by a distinctive interface. The equations were discretized using the volume of fluid (VOF) method, and the PIMPLE algorithm was used as the iteration method to reach a convergent solution [23].

The VOF method is based on the idea of a so-called fraction function C . C is defined as the integral of a fluid's characteristic function in the control volume, namely the volume of a computational grid cell. From a cell-volume averaged perspective, when a cell is empty of the sarin, the value of C is zero; when the cell is full of sarin, $C = 1$, and when the cell contains an interface between the sarin and the air volumes, $0 < C < 1$ [24].

4.3. Boundary conditions

The boundary conditions in the problem are the ceiling ventilation ducts and tunnels on both side of station. The ceiling ducts are defined with the inflow rate of $50 \text{ m}^3/\text{s}$ (based on Table 3), and the tunnels on both side of the station are defined with the outflow and inflow rates based on Figure 9.

4.4. Results

The results obtained in this section are presented for four cases, namely the case with no train service in the system, train arrival at the station, train departure from the station, and the case with successive train arrivals at and departures from the station.

4.3.1. No train service in system

Figure 11 shows the sarin dispersion throughout the station. It can be observed that 5 minutes after the sarin release, it is quickly dispersed across the station and reaches its maximum concentration after 20 minutes. Given the no-train service in the system, as well as the air flow direction of the main air handling unit of the station (Bl_1 fan based on Figure 3) and two injection shafts at both sides of

the station (B1₂ and B1₃ based on Figure 3), the sarin-contaminated air entered two tunnels on the two sides of the station.

Figure 12 shows the sarin concentration as a function of time at a height of 1 m above the platform and at the platform center. According to the figure, sarin reached its maximum concentration (approximately 9 mg/m³) after about 20 minutes. After this period, the sarin concentration gradually declined as most of the liquid sarin evaporated. Figure 13 shows the dose of sarin as a function of time in this scenario. A

comparison of this graph and LCT₅₀ reveals that, in the case with no train, the sarin dispersion was lethal after about 5 minutes, while after 10 minutes, the sarin dose reached LCT₅₀ and could kill 50% of the exposed people (based on Table 2, LCT₅₀ is the dose that for the exposure time, t, produces lethal effects in 50% of the exposed population). By considering the direction of the air flow on the platform, it was observed that the sarin concentration was quite insignificant on the second floor (ticket hall).

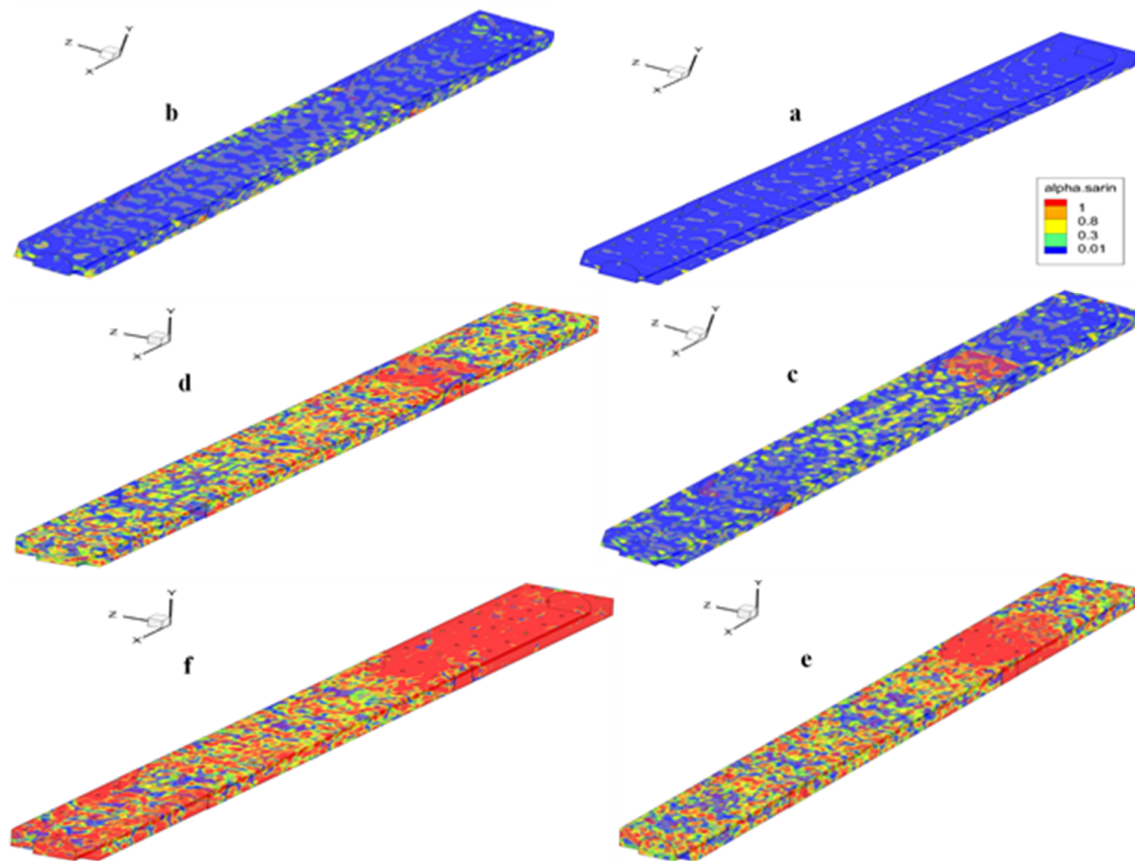


Figure 11. Concentration fields in platform at a: t = 5 min; b: t = 10 min; c: t = 12 min; d: t = 14 min; e: t = 18 min, and f: t = 30 min after release when there is no train service in the system.

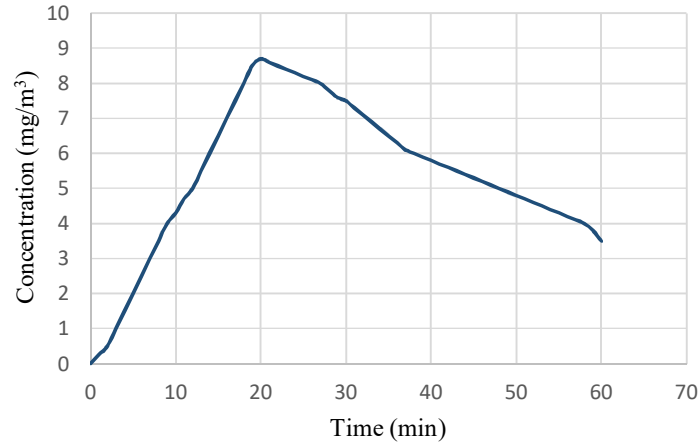


Figure 12. Average concentration of sarin 1 m above platform when there is no train in the system.

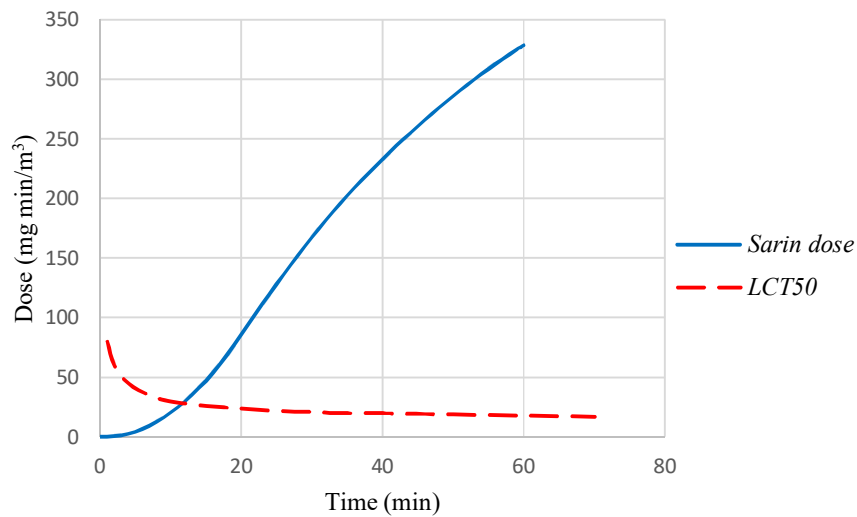


Figure 13. Average doses of sarin 1 m above platform when there is no train in the system.

4.3.2. Train arrival at station

The airflow caused by the piston action of the train upon its arrival at the station (Figure 9) was applied as the boundary condition of the sarin dispersion problem in the case without a train, and the effects of train piston effect on the sarin dispersion throughout the station were determined. Since the sarin concentrations were low at the beginning and end of the dispersion period, the results could not be properly analyzed. Therefore, the analyses were performed at the time of maximum sarin concentration (after 20 minutes, as shown in Figure 12). Figure 14 shows sarin dispersion across the station within the period from 20 to 22 minutes after the release (the speed-time graph showed that there was a 105-s period between the train exit from the previous station and its arrival at the studied station), as a train was

moving toward the studied station 20 minutes after release. In this scenario, as the train started moving from the previous station towards the studied station, no variations were made in the sarin dispersion conditions because the train was initially slow and far from the studied station. As the train reached its maximum speed and neared the station, the sarin concentration increased on one side of the station due to air flow through the station as a result of the train piston action and the train direction. Furthermore, the train arrival also caused sarin diffusion to the second floor (ticket hall). In fact, as the train arrived at the station, the air inside the tunnel flowed towards the platform, entered the ticket halls through the corridors, and then left the station through the ground-level entrances.

Figure 15 shows the sarin concentration as a function of time at a height of 1 m above the

platform and inside the ticket hall when a train entered the station 20 minutes after the initial release. It could be observed that the train entrance

to the station slightly decreased sarin concentration on the platform, and raised it up to $0.35 \text{ mg}/\beta^3$ in the ticket hall.

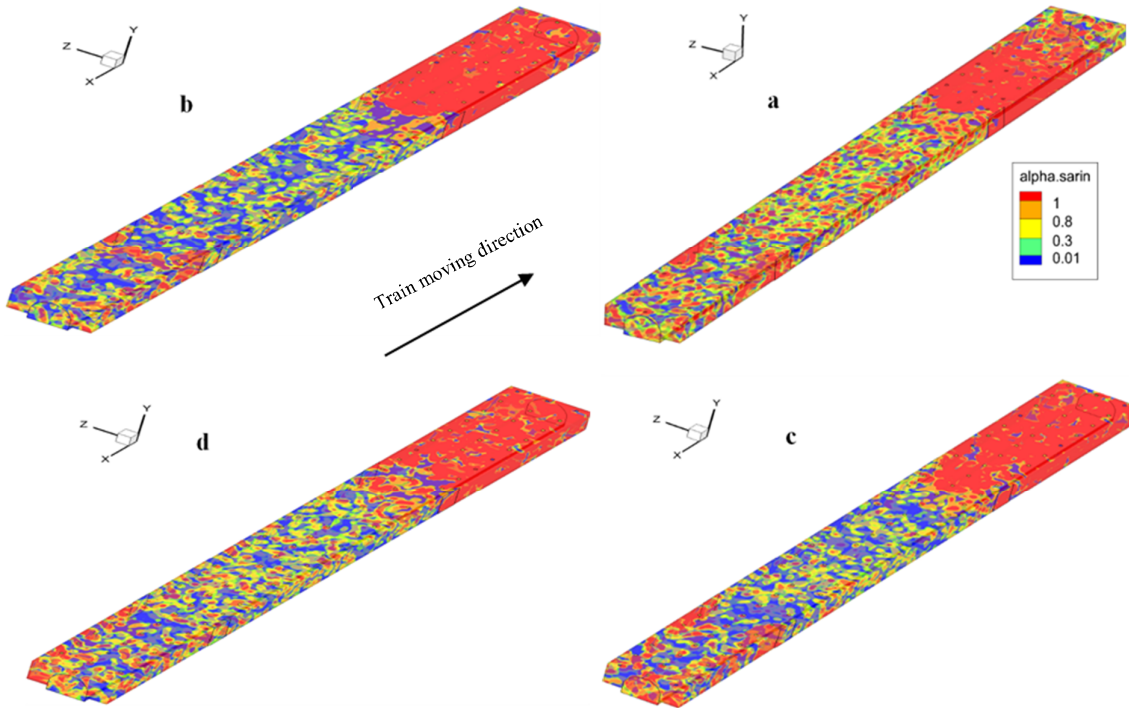


Figure 14. Concentration fields in platform at a: $t = 10 \text{ s}$; b: $t = 40 \text{ s}$; c: $t = 80 \text{ s}$, and d: $t = 100 \text{ s}$ after release.

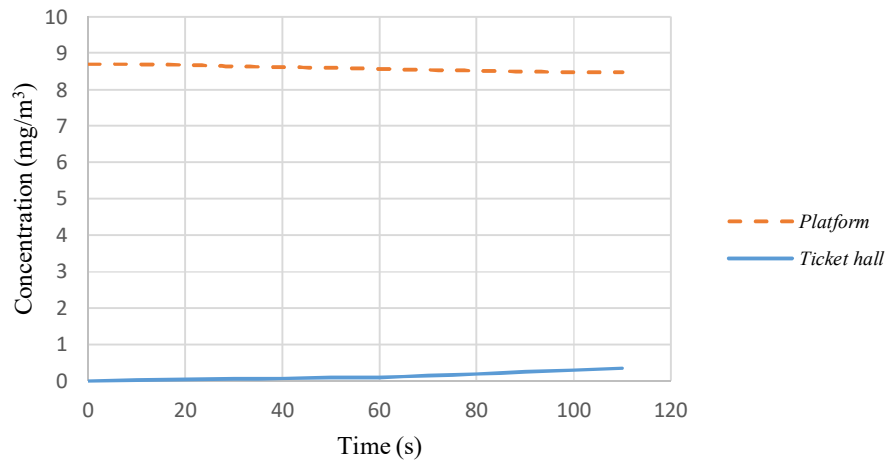


Figure 15. Average concentration of sarin 1 m above platform and ticket hall in the scenario of a train entering the station.

4.3.3. Train departure from station

In this scenario, similar to the previous one, the analyses were made for the period when the sarin concentration reached its maximum. Figure 16 shows sarin dispersion throughout the station in the period from 20 to 22 minutes after the release, when a train was leaving the station 20 minutes

after the release. According to the figure, the sarin concentration increased on one side of the station due to the air sucked into the station as a result of the piston effect and train movement as it left the station.

With the train leaving the station, the sarin concentration on the second floor (ticket hall) also

dropped to zero, which is due to the fresh air sucked into the ticket halls and platforms from outside through the station ground-level entrances.

Figure 17 shows the graph of sarin concentration as a function of time at a height of 1 m above the platform when the train was leaving the station 20 minutes after the initial release. It could be observed in the figure that as the train left the

station, the sarin concentration was reduced on the platform. There was a larger reduction of sarin concentration in this scenario than the train arrival scenario. This is due to the higher rate of air flow sucked from the station when the train left than the rate of air flow entering the station as the train arrived at the station (based on Figure 8).

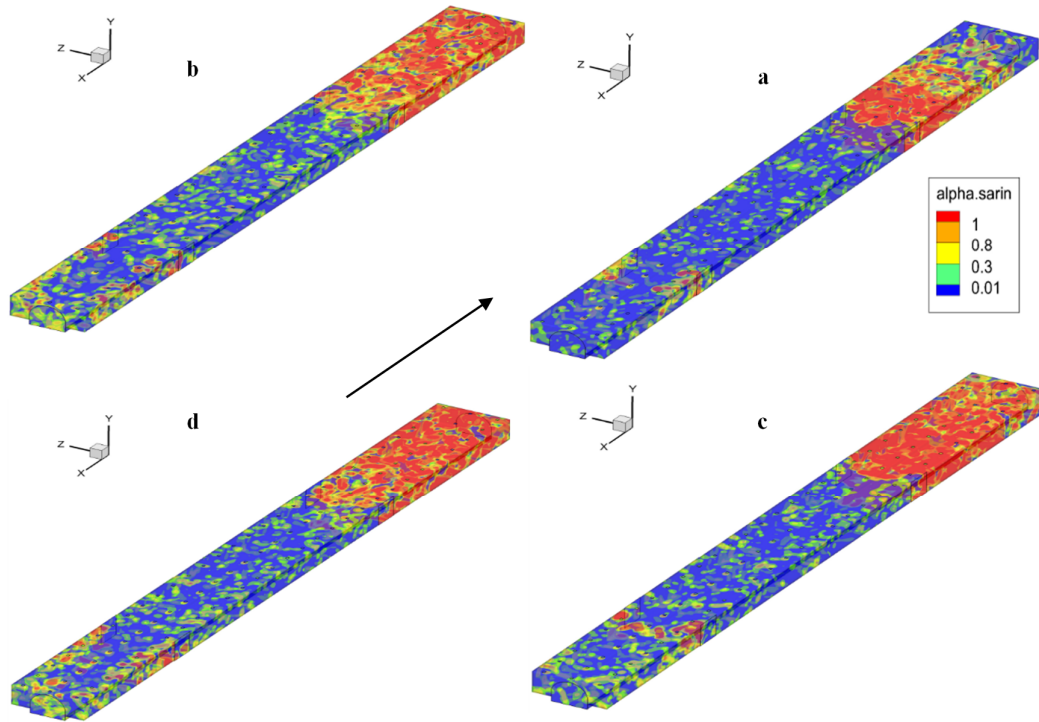


Figure 16. Concentration fields in platform at a: $t = 10$ s; b: $t = 40$ s; c: $t = 80$ s, and d: $t = 100$ s after release in the scenario of a train leaving the station.

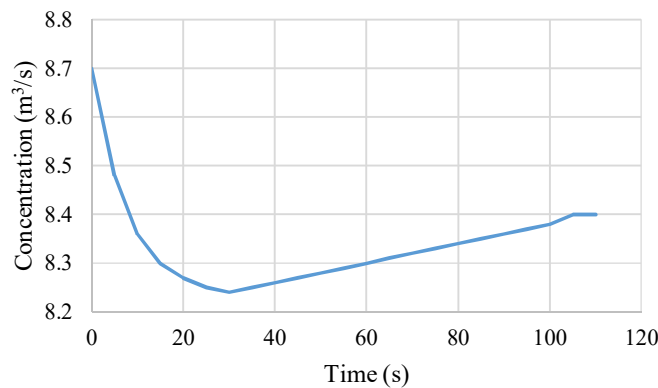


Figure 17. Average concentration of sarin 1 m above platform in the scenario of a train leaving the station.

4.3.4. Train arrival at and departure from station

The previous analyses concerned the train arrival and departure scenarios with no train traffic

through the station within the first 20 minutes from the release. This would not happen in the real-life situations, as there are train arrivals and departures at specified intervals in a real subway station. In order to simulate real situations more accurately,

some analyses were conducted for the case with multiple arrivals and departures at specific time intervals. In this scenario, it was assumed that one train arrived at the station every 5 minutes and left after a 2-minute stop. The modeling covered a 60-minute period starting from the sarin release. [Figure 18](#) shows the sarin concentration as a function of time at a height of 1 m above the platform on the second floor when there were arrivals at and departures from the station. When a train started moving to the station, the sarin concentration decrease in the platform because of sarin diffusion to the second floor and tunnel on the other side of the station. Similarly, when a train left the station, the sarin concentration also decreased in the platform because of fresh air suction to the station due to the train piston action. These arrival and departure times are indicated by the descending values in the graph. When the train arrived the studied station and left it and reached to

the next station, the concentration of sarin on the platform increased until the next train arrived the studied station. With successive train arrivals and departures, an insignificant amount of sarin also entered the second floor. The graph of the dose of sarin as a function of time is given in [Figure 19](#), which shows that train arrivals and departures at specific time intervals considerably reduced the dose of sarin on the platform. When this happens, after about 18 minutes, the sarin dose reached LCT_{50} and half of the exposed people. Furthermore, the dose of sarin on the second floor would not be high enough to be lethal. In fact, as a train arrived at the station, the resulting air circulation inside the station caused some of the sarin dispersed around the platform area to enter the second floor; when the train left the station, that portion of sarin was discharged from the second floor and re-entered the platform.

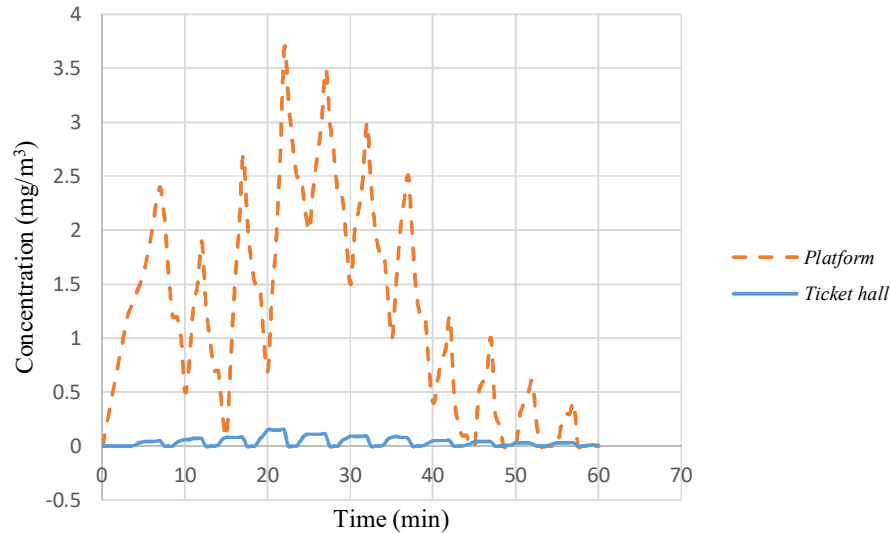


Figure 18. Average concentration of sarin 1 m above platform and ticket hall in the scenario of entering and leaving trains from the station.

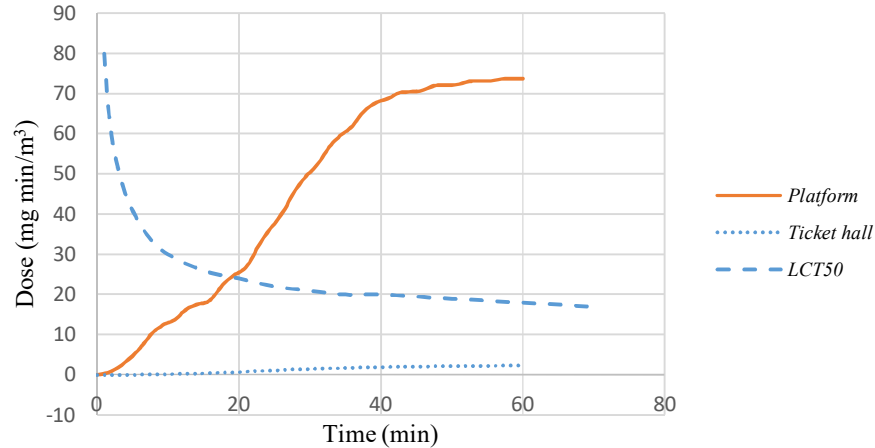


Figure 19. Average dose of sarin 1 m above platform and ticket hall in the scenario of entering and leaving trains from the station.

5. Conclusions

Dispersion of a chemical agent inside a subway station was numerically analyzed in a hypothetical scenario. In an analysis of the environmental conditions in a subway station, the train piston effect should be taken into account in addition to the ventilation system. In fact, the piston effect is the only factor discriminating between subway stations and other underground spaces when it comes to the analysis of their environmental conditions. There are several scenarios for launching a chemical attack on a subway station. This work considered sarin release through the ventilation system of the station.

- 5 minutes after sarin release in the no-train scenario, sarin was quickly dispersed throughout the station, and reached its maximum concentration after 20 minutes. Due to the type of the ventilation system, the sarin-contaminated air entered two tunnels on the two sides of the station. When there was no train, sarin dispersion became lethal after about 5 minutes, while it could kill 50% of the exposed individuals after about 10 minutes. The sarin concentration was quite insignificant on the second floor (ticket hall) due to the direction of air flow over the platform.
- With the sarin concentration at a maximum, the movement of a train toward the station caused the air to flow through the station as a result of the train piston effect and direction of train movement, increasing the sarin concentration on one side of the station. The train moving toward the station also caused sarin to enter the second floor (ticket hall). Train arrival at the station slightly decreased the sarin concentration on the

platform, and raised it up to 0.35 mg/m^3 in the ticket hall.

- With the sarin concentration at a maximum, the departure of a train from the station caused the air to be sucked from the station due to the train piston effect and direction of train movement, increasing the sarin concentration on one side of the station. The train departure from the station also reduced the sarin concentration to zero on the second floor (ticket hall), which was due to the fresh air sucked from outside through the ground-level entrances toward the ticket hall and platforms. As the train left the station, the sarin concentration on the platform was decreased. The reduction in sarin concentration was larger compared to that in the train arrival scenario. This is due to the fact that the rate of air flow sucked from the station as the train left was higher than the rate of air flow entering the station as the train arrived.
- Successive train arrivals at and departures from the station introduced an insignificant amount of sarin into the second floor. Arrivals and departures at specific time intervals considerably reduced the dose of sarin on the platform. These circumstances, after about 18 minutes, would put the life of half of the exposed individuals at risk. Furthermore, the dose of sarin in the second floor was not high enough to be lethal.
- Sarin release through the ventilation system is highly dangerous and lethal: about 0.5 L of sarin released in the ventilation system of the station would have severely adverse effects on many individuals, and lead to death. This is highly important, especially when the effect of ventilation chambers at the ground level is taken into consideration.

- The influences of the train piston effect on the station were both positive and negative. It was shown that while the negative effects were quite insignificant, the positive effects greatly contributed to lower casualties.
- Time is a key factor to save lives in the management of such incidents as chemical attacks on subway stations: reducing the attack detection time to 10 minutes saved the lives of 50% of the exposed individuals.

References

- [1]. Montazeri, M. (2010). Subway systems. Tehran: Tehran Urban and Suburban Railway Operation Co.
- [2]. Leikin, J.B., Thomas, R.G., Walter, F.G., Klein, R. and Meislin, H.W. (2002). A Review of Nerve Agent Exposure for the Critical Care Physician. *Critical Care Medicine*. 30 (10): 2346-2354.
- [3]. Sakurada, K. and Ohta, H. (2020). No promising antidote 25 years after the Tokyo subway sarin attack: A review. *Legal Medicine*, 47.
- [4]. TU, A.T. (2007). Toxicological and Chemical Aspects of Sarin Terrorism in Japan in 1994 and 1995. *Toxin Reviews*, 26, 231–274.
- [5]. Endregard, M., Reif, B.P., Vik, T. and Busmundrud, O. (2010). Consequence assessment of indoor dispersion of sarin—A hypothetical scenario. *Journal of Hazardous Materials*, 176, 381–388.
- [6]. Pflitsch, A., Brüne, M., Heinze, M. K., Ringeis, J., Agnew, B. and Steiling, B. (2013). Natural Ventilation as a Factor Controlling the Dispersal of Airborne Toxins in Subway Systems in a Disaster Situation. *Journal of Transportation Safety and Security*. 5 (1): 78-92.
- [7]. Spiegel, J., Brüne, M., Dering, N., Pflitsch, A., Qian, Z., Agnew, B. and Irving, M. (2014). Propagation of tracer gas in a subway station controlled by natural ventilation. *Journal of Heat Island Institute International*. 9 (2): 103-107.
- [8]. Gross, G. (2015). Dispersion scenarios for pollution release in an occupied underground station – a numerical study with a micro-scale and a multi-agent model. *Meteorologische Zeitschrift*. 24 (5): 511–524.
- [9]. Widiatmojo, A., Sasaki, K., Widodo, N.P., Sugai, Y., Yousefi Sahzabi, A. and Nguele, R. (2016). Predicting gas dispersion in large scale underground ventilation: A particle tracking approach. *Building and Environment*, 95, 171-181.
- [10]. Brüne, M., Spiegel, J. and Pflitsch, A. (2015). Tracer gas experiments in subways using an integrated measuring and analysis system for sulphur hexafluoride. *AMA Conferences 2015*. Nürnberg, Germany.
- [11]. Ma, L., Chen, B., Qiu, S., Li, Z. and Qiu, X. (2017). Agent-based modeling of emergency evacuation in a railway station square under sarin terrorist attack. *International Journal of Modeling, Simulation, and Scientific Computing*, 8(4).
- [12]. Feng, J.R., Gai, W.-m. and Yan, Y.-b. (2021). Emergency evacuation risk assessment and mitigation strategy for a toxic gas leak in an underground space: The case of a subway station in Guangzhou, China. *Safety Science*, 134.
- [13]. Dolezal, O. and Tomaskova, H. (2020). An agent-based simulation to minimize losses during a terrorist attack. *Applied science*, 10, 10.
- [14]. United states air force. (2008). Chemical and biological warfare overview. United states air force.
- [15]. Bide, R.W., Armour, S.J. and Yee, E. (2005). GB toxicity reassessed using newer techniques for estimation of human toxicity from animal inhalation toxicity data: new method for estimating acute human toxicity (GB). *Appl. Toxicol*, 25, 393-409.
- [16]. Handbook of Tehran metro system (Line 3). (2018). Tehran: Tehran urban and suburban railway co.
- [17]. Xue, P., You, S., Chao, J. and Ye, T. (2014). Numerical investigation of unsteady airflow in subway influenced by piston effect based on dynamic mesh. *Tunnelling and Underground Space Technology*, 40, 174-181.
- [18]. Kim, Y.J. and Kim, K.Y. (2007). Experimental and numerical analyses of train-induced unsteady tunnel flow in subway. *Tunnelling and Underground Space Technology*, 22, 166-172.
- [19]. Yuan-dong, H. and Wei, G. a.-N. (2010). A numerical study of the train-induced unsteady airflow in a subway tunnel with natural ventilation ducts using the dynamic layering method. *Journal of hydrodynamics*. 22 (2): 164-172.
- [20]. Huang, Y., Hong, T.H. and Kim, C.N. (2012). A numerical simulation of train-induced unsteady airflow in a tunnel of Seoul subway†. *Journal of Mechanical Science and Technology*. 26 (3): 785-792.
- [21]. Hoffman, K.A. and Chiang, S.T. (2000). *Computational Fluid Dynamics Vol I*. Kansas: engineering Education System.
- [22]. Moshari, S., Nikseresht, A. and Mehryar, R. (2014). Numerical analysis of two and three dimensional buoyancy driven water-exit of a circular cylinder. *International Journal of Naval Architecture and Ocean Engineering*, 6, 219-235.
- [23]. Wilcox, D.C. (1993). *Turbulence Modeling for CFD*. DCW Industries.
- [24]. Hirt, C.W. and Nichols, B.D. (1981). Volume of fluid (VOF) method for the dynamics of free boundaries. *Journal of Computational Physics*. 39 (1): 201-225.

مدلسازی انتشار گاز سارین در ایستگاه مترو در یک سناریوی فرضی با استفاده از دینامیک سیالات محاسباتی

سید محمد حسینی دشتیخوانی، سید حسن مدنی* و کوروش شهریار

دانشکده مهندسی معدن دانشگاه صنعتی امیرکبیر تهران، ایران

ارسال ۲۰۲۲/۰۱/۲۶، پذیرش ۲۰۲۲/۰۲/۰۹

* نویسنده مسئول مکاتبات: hmadani@aut.ac.ir

چکیده:

هدف اصلی این مطالعه، مدلسازی انتشار گاز سارین در ایستگاه مترو است. مدلسازی در یک سناریوی فرضی و با استفاده از دینامیک سیالات محاسباتی انجام گرفته است. در بررسی شرایط محیطی فضاهای زیرزمینی، تنها عاملی که ایستگاه‌های مترو را از سایر فضاهای زیرزمینی متمایز می‌کند، اثر پیستونی قطار است، لذا بررسی‌ها در دو حالت کلی بود و نبود قطار در سیستم انجام شده است. برای مدلسازی انتشار سارین، فرض شده که حدود ۰/۵ لیتر سارین از طریق سیستم تهویه اصلی وارد فضای ایستگاه شود. نتایج نشان دهنده آن است که در حالت نبود قطار در سیستم، بعد از حدود ۲۰ دقیقه از انتشار سارین در ایستگاه، غلظت گاز به ۸/۹ میلی‌گرم در متر مکعب و دوز به ۸۰ میلی‌گرم دقیقه در متر مکعب می‌رسد که این مقادیر بسیار خطرناک و کشنده بوده و صدمات شدید و کشنده برای افراد در معرض در پی خواهد داشت. این موضوع با توجه به وجود اتاقک‌های ورودی هوای ایستگاه در سطح خیابان بسیار حائز اهمیت است. همچنین نتایج نشان‌دهنده آن است که اثر پیستونی قطار باعث کاهش غلظت و دوز سارین در ایستگاه خواهد شد به طوری که با ورود و خروج قطار از ایستگاه، دوز سارین به مقدار ۲۵ میلی‌گرم دقیقه در متر مکعب می‌رسد و تلفات کاهش می‌یابد. در نهایت نتایج نشان دهنده آن است که زمان در مدیریت این نوع حوادث و کاهش تعداد تلفات یک عامل بسیار مهم و کلیدی است.

کلمات کلیدی: سارین، حمله شیمیایی، اثر پیستونی، دینامیک سیالات محاسباتی، ایستگاه مترو.
